https://doi.org/10.1016/j.amc.2020.125765

The impact of contact patterns of sexual networks on Zika virus spread: a case study in Costa Rica

XiaoFeng Luo[a,b,c,d,e], Zhen Jin[b,a,c,d,e,*], Daihai He[f]

[a]*School of Computer and Information Technology, Shanxi University, Taiyuan 030006, Shanxi, China*
[b]*Complex System Research Center, Shanxi University, Taiyuan 030006, Shanxi, China*
[c]*Shanxi Key Laboratory of Mathematical Techniques and Big Data Analysis on Disease Control and Prevention, Shanxi University, Taiyuan 030006, Shanxi, China*
[d]*Key Laboratory of Computational Intelligence and Chinese Information, Processing of Ministry of Education, Taiyuan 030006, China*
[e]*Key Discipline of Computer Science and Technology of Double-First-Class Project of Shanxi Province, Taiyuan 030006, China*
[f]*Department of Applied Mathematics, The Hong Kong Polytechnic University, Hung Hom, Kowloon, Hong Kong (SAR), China*

Abstract

The impact of Zika virus (ZIKV) is a global public health issue and its severity is ongoing. It is primarily transmitted via mosquitoes and sexual contacts. Sexual transmission experiences a longer period and strongly depends on the topological structure of sexual networks. However, relatively little work has been done to explore the characteristics of ZIKV infection in sexual networks, and further control ZIKV by changing contact patterns between individuals. In this paper, using the settings of Costa Rica as a case study, we developed a heterosexual network-based model, to study the effect of changing the degree heterogeneity by the measure of deleting the sexual contacts of individuals with small number but large degree in the sexually active places at different time, on ZIKV spread. We obtained a threshold time, which is later than the peak time of ZIKV infected cases. If applied prior to the threshold time, the measure will inhibit ZIKV infection and lower the final size; surprisingly if past the threshold time, the measure will boost ZIKV infection and increase the final size. In addition, our model yields higher cumulative infection among females, which is in line with observations. Our results provide some guidelines for preventing and controlling mosquito-human and sexual transmissions against ZIKV, particularly for countries with a high rate of sexually transmitted infections.

Keywords: Zika virus, sexual contact patterns, network, time threshold of deleting nodes with large degree

1. Introduction

Zika virus (hereafter referred to ZIKV) has been a global concern since the outbreak in Brazil in March 2015 [1]. ZIKV, similar to dengue, is an arthropod-borne flavivirus, vectored by infected female mosquitoes of genus Aedes. Besides mosquitoes, ZIKV can also be transmitted by sexual contacts [2]. In general, approximately 20% of ZIKV infections [3] (50% or 66% in French Polynesia 2014-2015 [4]) shows mild symptoms including mild fever, rash, conjunctivitis and joint pain. Recent research also indicates that the virus is closely associated with neurological disorders, especially microcephaly [5]. Unfortunately, there are no feasible treatment and vaccine for ZIKV.

ZIKV was first isolated from the serum of a febrile sentinel rhesus monkey in the Zika forest of Uganda in 1947 and then discovered from Aedes africanus mosquitoes in the same forest in 1948 [6]. It was first identified in humans from the serum of east African residents in 1952 [7]. In April 2007, cases outside Africa and Asia were reported on Yap Island in the southwestern Pacific Ocean [8]. Since then, the outbreak of disease ZIKV induces has become serious. In October 2013, a severe outbreak hit French Polynesia and caused an estimated 28,000 cases [9]. Subsequently, an outbreak started in Brazil in March 2015 and swept across South and Central America with more than 140,000 suspected and confirmed cases by the end of February 2016 [10, 11]. WHO immediately declared ZIKV as a Public

*Corresponding author.
Email address: jinzhn@263.net (Zhen Jin)

Health Emergency of International Concern on February 1, 2016. CDC Emergency Operations Center also declared actions for moves to the highest level of activation on February 3, 2016 [12]. ZIKV has been detected in semen, blood and other body fluids and especially stays longer time in semen [13, 14, 15]. The two main routes of ZIKV transmission are mosquito bites and sexual contacts. Recently, there have been many research on ZIKV outbreak using mathematical models [3, 10, 11, 16, 17, 18, 19]. Most of them treated mosquito-human transmission as the dominant form of ZIKV transmission [16, 17, 18] and suggested some control measures [19]. Only a few studies considered the two transmission routes simultaneously [3, 10, 11, 20].

Gao *et al.* developed a deterministic model with both mosquito-human and sexual transmissions and studied the contribution of the two transmission routes to the basic reproduction number and the attack rate [10]. Based on Gao's work, Maxian *et al.* built a sex- or age-structured model to further explore the contribution of sexual transmission to ZIKV spread under different conditions [3]. Moreover, Agusto *et al.* established a model with both mosquito-human and sexual transmissions and analyzed the dynamical behavior of the model [20]. All the above studies were based on the well-mixed-population by assuming that each individual has the same number of sexual partners. However, in general, the majority of the married individuals have one heterosexual partner; children and the elderly may have zero sexual partners; sexually active individuals (middle age) especially in countries with a high rate of sexually transmitted infections may have more sexual partners. Research has already indicated that, the discrepant contact patterns (or degree heterogeneity) between individuals within population have great impacts on disease spread [21, 22, 23, 24]. In order to find out the quantifiable impacts and further propose control measures, it is important to establish a network-based mathematical models, in which each individual is represented by a node and each contact by an edge.

However, from the research done so far and to the best of our knowledge, it clearly shows that the network-based model to study the impact of contact patterns on ZIKV spread has not been carried out yet. Hence, in this paper, we established a heterosexual network-based model to explore effects of changing degree (contact or edge) heterogeneity at different time on ZIKV spread. We used Costa Rica as a case study, due to the availability of ZIKV data, and the high rate of sexually transmitted infections in that country. The age factor is considered by grouping individuals in sexually inactive age (children and the elderly) as nodes of degree zero (0), and individuals in the sexually active age as nodes of degree more than zero (0). We estimate the degree distribution and the threshold time of changing the degree heterogeneity through measures of supervising, isolating and closing sexually active places to cut off sexual contacts of individuals with a greater number of sexual partners. Also, we quantified that the probabilities of one female or male individual is connected to an opposite sex infected individual via one sexual contact during ZIKV spread, which causes higher cumulative and infected cases in females. Our work will help researchers and health authorities to gain a better understanding of the evolution of ZIKV in sexually active regions or countries and formulate comprehensive measures against ZIKV. The rest of this paper is organized as follows; Section 2 elaborates on the methods, Section 3 contains the results and finally Section 4 gives the discussions and conclusions.

2. Material and methods

2.1. The network with sexual contacts and mosquito-human contacts

ZIKV can exist in semen much longer than in blood and other body fluids [13, 14, 15]. It means that sexual transmission has a longer infectious duration than mosquito-human transmission. Thus, sexual transmission could play a crucial role during ZIKA outbreak. Since the unrecognized same-sex sexual activity is of a small proportion in most countries and the outbreak of ZIKA in specific regions lasts typically short, we consider a network with heterosexual contacts and human-mosquito contacts (Figure 1), to study the effects of network degree heterogeneity on ZIKV spread. In the following, we first introduce the degree distribution of the heterosexual network.

According to the empirical observations [22], the general sexual-contact networks are referred as the bipartite scale-free (SF) networks. In such networks, the number k of contacts of a node with other nodes—the degree k of this node—follows a power-law distribution, $p_k \sim k^{-\gamma}$. The expression of the degree distributions for both male and female nodes are respectively

$$p_k^m \sim k^{-\gamma^m} \text{and } p_k^f \sim k^{-\gamma^f}, \quad k = k_0, \cdots, k_{max}, \tag{1}$$

where k_0 stands for the minimum degree ($k_0 > 0$) and k_{max} stands for the maximum degree with $\sum_{k=k_0}^{k_{max}} p_k^m = 1$ and $\sum_{k=k_0}^{k_{max}} p_k^f = 1$. Note that for the power-law distribution of Eq. (1) the minimum degree k_0 of network is more than

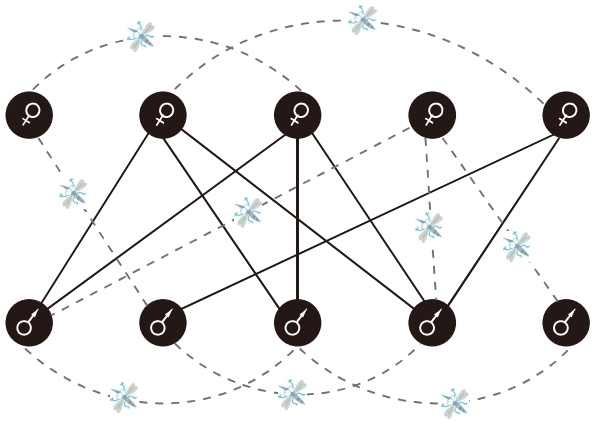

Figure 1: Representation of the whole contact network with heterosexual contacts (black solid line) and human-mosquito contacts (gray dashed line) which connects the isolated individuals to others. In such a network, N_k^m (N_k^f) represents male (female) nodes with k ($0 \le k \le k_{max}$) female (male) partners.

0; that is, the size of nodes based on the power-law distribution is only the size of individuals with sexual partners (or contacts). However, for ZIKV, nodes without sexual contacts—children and the elderly, participate in mosquito-human transmission, thus degree of which is set to 0. In order to consider the two type nodes without and with sexual contacts at the same time, we normalize the two types of nodes in the total population according to demographic data in Costa Rica from World Bank 2016 [25] in Section 2.3, and obtain the degree distributions of the heterosexual network.

Since mosquitoes randomly bite humans, they connect the individuals with sexual contacts and individuals without sexual contacts (isolated individuals) to form the whole network with sexual contacts and the mosquito-human contacts, as shown in Figure 1.

The heterosexual bipartite network (of size N) — network between humans in Figure 1 consists of two gender groups—the male group (of size N^m) and the female group (of size N^f). From the viewpoint of the degree of nodes, the network can also be divided into $k_{max}+1$ groups. Each group is a set of nodes with the same degree k ($0 \le k \le k_{max}$) and its size is N_k, satisfying $N = N^m + N^f = \sum_{k=0}^{k_{max}} N_k$. Additionally, N_k^m and N_k^f depict the total size of the male nodes and the female nodes in the group of N_k size, satisfying

$$N_k = N_k^m + N_k^f, \quad N^m = \sum_{k=0}^{k_{max}} N_k^m, \quad N^f = \sum_{k=0}^{k_{max}} N_k^f, \quad k = 0, 1, \cdots, k_{max}.$$

The degree distribution and the average degree of network are respectively denoted by

$$p_k = \frac{N_k^m + N_k^f}{N^m + N^f}, \quad \langle k \rangle = \sum_{k=0}^{k_{max}} k p_k, \quad k = 0, 1, \cdots, k_{max}.$$

Now let $\langle k^2 \rangle / \langle k \rangle = \sum_{k=0}^{k_{max}} k^2 p_k / \sum_{k=0}^{k_{max}} k p_k$ be the basis to measure the level of heterogeneity.

The relative degree distributions and the relative average degrees of the male and female groups are respectively

$$p_k^m = \frac{N_k^m}{N^m}, \quad \langle k \rangle_m = \sum_{k=0}^{k_{max}} k p_k^m, \quad k = 0, 1, \cdots, k_{max},$$

and

$$p_k^f = \frac{N_k^f}{N^f}, \quad \langle k \rangle_f = \sum_{k=0}^{k_{max}} k p_k^f, \quad k = 0, 1, \cdots, k_{max}.$$

Denoting the fraction of the female nodes in the heterosexual networks by θ, $\theta = N^f/N$, the average degree is represented as

$$\langle k\rangle = (1-\theta)\langle k\rangle_m + \theta\langle k\rangle_f.$$

In addition, in the heterosexual networks, there exists the following closure relation

$$N^m\langle k\rangle_m = N^f\langle k\rangle_f. \tag{2}$$

It means that the number of edges ending at the male group (of size N^m) equals the number of edges ending at the female group (of size N^f).

2.2. A heterosexual network-based model with mosquito-human transmission

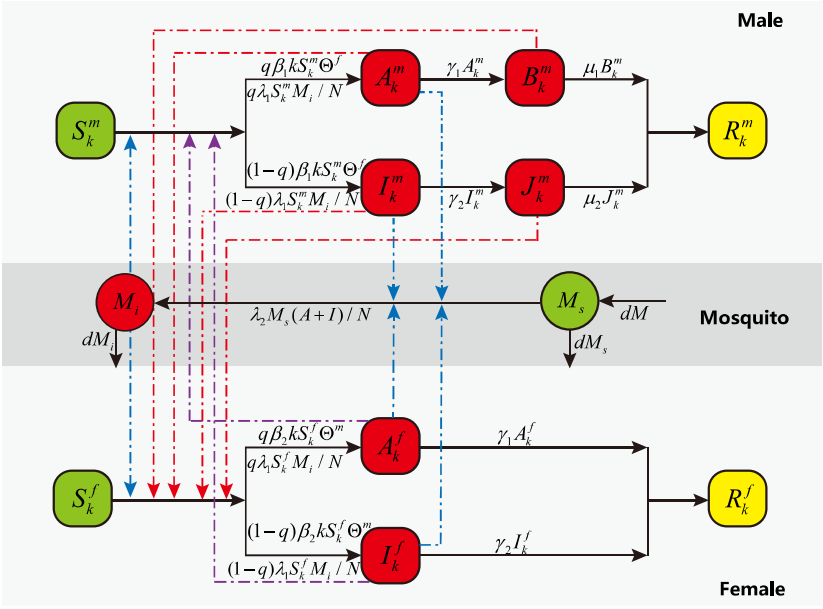

Figure 2: Flow diagram for ZIKV spread involving mosquito-human and sexual transmission. Solid squares and circles represent humans and mosquitoes respectively, among which the green and yellow are non-infectious and the red are infectious. Black solid arrows describe the progression of infection. Red dashed arrows show direction of male-to-female transmission, purple dashed arrows show direction of female-to-male transmission and blue dash-dotted lines show direction of transmission between humans and mosquitoes. S_k^m (S_k^f), A_k^m (A_k^f), I_k^m (I_k^f) and R_k^m (R_k^f) represent the number of nodes with degree k, gender male (female) and state of susceptible (S), asymptomatic infected (A), symptomatic infected (I)—both A and I with virus in semen, blood and other body fluids, and recovered (R), respectively; B_k^m, J_k^m represent the number of nodes with degree k, gender male and state of asymptomatic infected (B), symptomatic infected (J) both with virus only in semen; M_s and M_i represent the number of susceptible and infected mosquitoes, respectively.

To investigate the effects of the degree heterogeneity of the heterosexual network on ZIKV spread, based on the mean-field theory [21], we developed a mosquito-human and heterosexual network-based model. The flow chart is shown in Figure 2.

Since ZIKV can exist in semen much longer than in blood and other body fluids [13], the male nodes have additional time to transmit ZIKV. We assume that male nodes of degree k ($0 \le k \le k_{max}$) may experience states from susceptible (S) to asymptomatic infected (A) or symptomatic infected (I) both with virus in semen, blood and other body fluids to asymptomatic infected (B) or symptomatic infected (J) both with virus only in semen to recovered (R).

The number of each state is respectively represented by S_k^m, A_k^m, I_k^m, B_k^m, J_k^m and R_k^m. The female nodes of degree k ($0 \le k \le k_{max}$) may only experience state from susceptible (S) to asymptomatic infected (A) or symptomatic infected (I) both with virus in blood and other body fluids to recovered (R), and the number of each state is denoted by S_k^f, A_k^f, I_k^f and R_k^f, respectively. According to Section 2.1, these numbers of male and female nodes with different degrees and states satisfy

$$\begin{aligned} N = N^m + N^f &= \sum_{g\in\{m,f\}} S^g(t) + A^g(t) + I^g(t) + R^g(t) + B^m(t) + J^m(t) \\ &= \sum_{g\in\{m,f\}} \sum_k \Big(S_k^g(t) + A_k^g(t) + I_k^g(t) + R_k^g(t) + B_k^m(t) + J_k^m(t) \Big). \end{aligned} \tag{3}$$

For mosquito population, M_s and M_i depict the numbers of the susceptible and infected mosquitoes, respectively. We assume that, the birth rate d of mosquitoes is equal to the death rate, i.e., the total number M of mosquitoes is kept constant, $M = M_s + M_i$. A mosquito may progress from susceptible (M_s) to infected (M_i).

Table 1: Parameters in model (4)

Term	Meaning	Range	Value	Reference
θ	The proportion of the female in the human population		0.5	World Band Group[26]
q	Proportion of individuals who are asymptomatic after infection (per week)		0.82	[3, 10]
β_1	Transmission rate from the infected female to the susceptible male (per week)	0.221-0.235	0.228	Estimated
β_2	Transmission rate from the infected male to the susceptible female (per week)	0.111-0.118	0.115	Estimated
λ_1	Transmission rate from infected mosquito to susceptible human (per week)	0.510-0.528	0.519	Estimated
λ_2	Transmission rate from infected human to susceptible mosquito (per week)	0.510-0.528	0.519	Estimated
$1/\gamma_1$	Mean duration of state A (weeks)	5/7-9/7	1	Assumed
$1/\gamma_2$	Mean duration of state I (weeks)	5/7-9/7	1	[27]
$1/\mu_1$	Mean duration of state B (weeks)	50/7-60/7	55/7	Assumed
$1/\mu_2$	Mean duration of state J (weeks)	50/7-60/7	55/7	[27]
d	Natural birth and death rate of mosquitoes (per week)	7/45-7/55	7/50	[27, 28]
M	The size of mosquitoes population	2.008e6-2.048e6	2.028e6	Estimated

According to the model description and the parameters in Table 1, we developed a set of $10(k_{max}+1)+2$ ordinary differential equations in the given heterosexual network with mosquito-human contacts, which falls into male, female

human subpopulation and mosquito population.

The male subpopulation

$$\begin{cases} \dot{S}_k^m(t) &= -\beta_1 k S_k^m(t)\Theta^f(t) - \lambda_1 S_k^m(t) M_i(t)/N, \\ \dot{A}_k^m(t) &= q\beta_1 k S_k^m(t)\Theta^f(t) + q\lambda_1 S_k^m(t) M_i(t)/N - \gamma_1 A_k^m(t), \\ \dot{I}_k^m(t) &= (1-q)\beta_1 k S_k^m(t)\Theta^f(t) + (1-q)\lambda_1 S_k^m(t) M_i(t)/N - \gamma_2 I_k^m(t), \\ \dot{B}_k^m(t) &= \gamma_1 A_k^m(t) - \mu_1 B_k^m(t), \\ \dot{J}_k^m(t) &= \gamma_2 I_k^m(t) - \mu_2 J_k^m(t), \\ \dot{R}_k^m(t) &= \mu_1 B_k^m(t) + \mu_2 J_k^m(t). \end{cases} \qquad k = 0, 1, \cdots, k_{max} \tag{4a}$$

The female subpopulation

$$\begin{cases} \dot{S}_k^f(t) &= -\beta_2 k S_k^f(t)\Theta^m(t) - \lambda_1 S_k^f(t) M_i(t)/N, \\ \dot{A}_k^f(t) &= q\beta_2 k S_k^f(t)\Theta^m(t) + q\lambda_1 S_k^f(t) M_i(t)/N - \gamma_1 A_k^f(t), \\ \dot{I}_k^f(t) &= (1-q)\beta_2 k S_k^f(t)\Theta^m(t) + (1-q)\lambda_1 S_k^f(t) M_i(t)/N - \gamma_2 I_k^f(t), \\ \dot{R}_k^f(t) &= \gamma_1 A_k^f(t) + \gamma_2 I_k^f(t). \end{cases} \qquad k = 0, 1, \cdots, k_{max} \tag{4b}$$

The mosquito population

$$\begin{cases} \dot{M}_s(t) &= dM - \lambda_2 M_s(t)(A(t) + I(t))/N - dM_s(t), \\ \dot{M}_i(t) &= \lambda_2 M_s(t)(A(t) + I(t))/N - dM_i(t). \end{cases} \tag{4c}$$

where

$$\Theta^m(t) = \frac{\sum_{k'} \left(k' A_{k'}^m(t) + k' I_{k'}^m(t) + k' B_{k'}^m(t) + k' J_{k'}^m(t) \right)}{\langle k \rangle_m N^m}, \tag{5}$$

and

$$\Theta^f(t) = \frac{\sum_{k'} \left(k' A_{k'}^f(t) + k' I_{k'}^f(t) \right)}{\langle k \rangle_f N^f}, \tag{6}$$

with $\langle k \rangle_m N^m = \sum_l l N_l^m$ and $\langle k \rangle_f N^f = \sum_l l N_l^f$. The quantity $\Theta^m(t)$ ($\Theta^f(t)$) represents the probability that any given contact of female (male) individuals is linked to an infected male (female) individual [21].

2.3. The degree distribution of the heterosexual network

In what follows, we determine the distribution of the heterosexual network representing the human population, which is divided into female and male subpopulations based on gender. Firstly, we note that not all individuals of all age groups participate in sexual transmission. The demographic data in Costa Rica from World Bank 2016 [25], indicates that 22% of population are 0-14 years, 69% are between the ages 15-64 and 9% are more than 65 years (see Figure 3). Among these age groups, people at 0-14 years and more than 65 years are considered to be sexually inactive [3], and they are only involved in the mosquito-human transmission. Therefore, we set the degree of these isolated individuals to 0. The remaining 69% is sexually active who takes part in both sexual and mosquito-human transmissions, and they form the sexual-contact network of which the degree distribution follows power-law distribution of Eq. (1) with degree more than 0 (see Section 2.1). Secondly, the work [10, 29], indicates that sexually active individuals mostly have about two sexual partners (contacts) on average, and if averaging on sexually inactive and active individuals, one has about one sexual partner (contact); that is, the average degree of nodes only with sexual contacts is approximately 2 and the average degree of all nodes is approximately 1. Thirdly, according to report [30], the maximum number of opposite-sex partners of individuals during 15-44 years are 15 or more in the Americas, but the number of individuals with a degree more than 15 are low. Hence, we assume the maximum number of opposite-sex partners an individual may have in his or her life time in Costa Rica are 15, which is the maximum degree k_{max} of the network. Last but not the least, according to the demographic data from World Bank Group 2016 [26], the proportion θ of the female in Costa Rica has $\theta = 0.5$; that is a 1:1 sex ratio.

Within the constraints of the above assumption of the average sexual partners, the maximum degree k_{max} and sex ratio, based on (1) and the configuration model [31], the power exponent is set as $\gamma^m = 2.07$ and $\gamma^f = 2.12$ (where

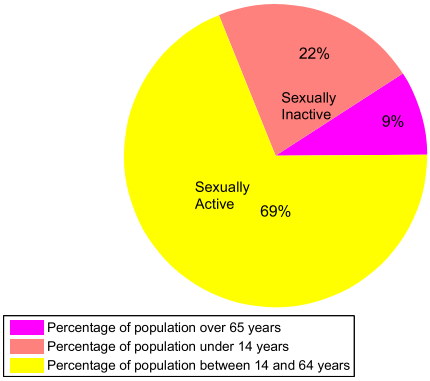

Figure 3: Age and sexual activity distributions in Costa Rica 2016 [25].

$\gamma^m < \gamma^f$ and the difference is small according to [22]), so the average degree of the obtained degree distribution (the inset in Figure 4) of the sexual-contact network only in terms of sexually active nodes satisfies $\langle k\rangle_m \approx \langle k\rangle_f \approx 2.0$. In order to include sexually inactive nodes, we normalize the sexual inactive and active nodes based on the their proportions of 31% and 69% of all nodes in Figure 3, to obtain the degree distribution of the heterosexual network with isolated nodes in Table 2 and Figure 4. The average degree is approximately 1.4, $\langle k\rangle_m \approx \langle k\rangle_f \approx 1.4$. Although the obtained heterosexual network is not the real network in Costa Rica (which is indeed difficult to obtain), it provides some guidelines for controlling ZIKV.

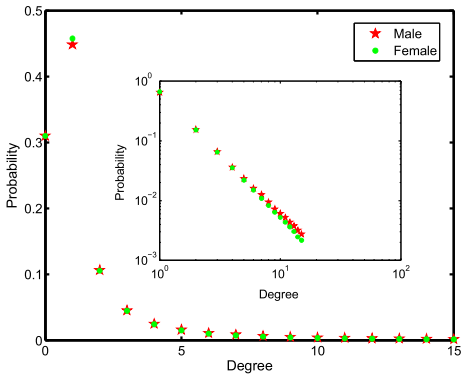

Figure 4: The degree distributions of the heterosexual network and the heterosexual network without isolated nodes in the inset.

2.4. MCMC algorithm

Next, according to [32, 33], we introduce the adaptive Metropolis-Hastings (M-H) algorithm of Markov Chain Monte Carlo (MCMC) simulations based on model (4). As the quality of the time series data is poor, we choose the limit cumulative cases of the reported ZIKV data in Costa Rica 2016, from Pan American Health Organization [34].

The following relationship exists between the reported cumulative cases $y(t)$ and the values $y^*(t)$ obtained from model (4) via ODE function in MATLAB

$$y(t) = y^*(t) + \varepsilon, \quad t = 0, \cdots, 19,$$

Table 2: The generated network degree distribution

Degree	0	1	2	3	4	5	6	7
Female Probability(p^f)	0.3100	0.4575	0.1057	0.0448	0.0244	0.0152	0.0104	0.0075
Male Probability(p^m)	0.3100	0.4485	0.1064	0.0454	0.0249	0.0161	0.0110	0.0087
Degree	8	9	10	11	12	13	14	15
Female Probability(p^f)	0.0057	0.0044	0.0036	0.0030	0.0025	0.0021	0.0017	0.0015
Male Probability(p^m)	0.0065	0.0050	0.0042	0.0036	0.0030	0.0026	0.0022	0.0019

where

$$y^*(t) = \sum_{t=0}^{19} \sum_{k=0}^{k_{max}} \left[I_k^m(t) + I_k^f(t) \right] \tag{7}$$

with $y(0) = y^*(0)$ and ε is assumed to follow the standard normal distribution $N(0, \sigma^2)$ ($\sigma = 0.1$). If we denote the parameter vector by $\Theta = (\beta_1, \beta_2, \lambda, M)$ with assumption $\lambda = \lambda_1 = \lambda_2$, the maximum likelihood function for the data $Y = \{y(t)\}_0^{T=19}$ has

$$L(Y|\Theta) = \prod_{t=0}^{T} \frac{1}{\sqrt{2\pi}\sigma} exp\left(-\frac{[y(t) - y^*(t)]^2}{\sigma^2} \right). \tag{8}$$

Then, the joint posterior distribution of the parameters is $P(\Theta|Y) \propto L(Y|\Theta)P(\Theta)$. For many biological models, one may only know the fact that the parameters of model are more than zero, so non-information prior distribution is adopted [33]. They generally assume $P(\Theta) \propto constant$, so the joint posterior distribution of the parameters becomes

$$P(\Theta|Y) \propto L(Y|\Theta). \tag{9}$$

In order to estimate model parameters, at each iteration, given the initial value $\Theta(0)$ we update the sample Θ^* by random walk [33] with the maximum walk values $\omega = (8 \times 10^{-4}, 8 \times 10^{-4}, 8 \times 10^{-4}, 1 \times 10^3)$. Then, with respect to the new parameters Θ^*, we calculate the cumulative cases of model (4) based on Eq. (7) to get the posterior likelihood $P(\Theta^*|Y)$ based on Eq. (8) and (9). The new values Θ^* of parameters will be accepted with probability

$$\min\left(1, \frac{P(\Theta^*|Y)}{P(\Theta|Y)}\right).$$

The corresponding algorithm is shown in Table 3 according to [33].

Table 3: The MCMC Algorithm [33]

Input: The total number of iterations *Iter*; The burn-in time *Bur*; The maximum walk values ω in random walk;
Output: The sample Θ from *Bur* to *Iter*;

1 Input the initial values of parameters $\Theta(0)$;
2 Calculate $P(\Theta(0)|Y)$ based on Eq. (8) and (9);
3 **For each** $i = 1$: (*Iter*) **do**
4 Get the new parameter Θ^*, $\Theta^* = \Theta(i-1) + \omega. \times [2 \times rand(1,4) - 1]$;
5 Calculate $P(\Theta^*|Y)$ based on Eq. (8) and (9);
6 With probability
$$\min\left(1, \frac{P(\Theta^*|Y)}{P(\Theta|Y)}\right)$$
Set $\Theta(i) = \Theta^*$;
Otherwise $\Theta(i) = \Theta(i-1)$.
7 **end**

3. Results

3.1. The parameter estimation

Costa Rica is a country in Central America and has two weather changes - dry season (November-April) and wet season (May-November) with stable temperatures. For data reliability, we select data between April 12th 2016 and August 24th 2016 [34] (blue circles in Figure 6). During this initially short period (19 weeks) there is no intervention on mosquito and hence we assume the size of the mosquito population is constant. Also, there exists no cure, treatment and no vaccine for ZIKV during this period.

In Table 1, for the easily obtained parameters γ_2, μ_2 and d, we fix $1/\gamma_2 = 1$ (range : $5/7, 9/7$), $1/\mu_2 = 55/7$ (range : $50/7, 60/7$) and $d = 7/50$ (range : $7/45, 7/55$) according to [27, 28]. For the parameters γ_1 and μ_1, there are no scientific references but the male asymptomatic or symptomatic individuals experience similar duration from infected to recovered [13]. We therefore assume $1/\gamma_1 = 1/\gamma_2$ and $1/\mu_1 = 1/\mu_2$. For the parameters $\beta_1, \beta_2, \lambda_1, \lambda_2$ and M, not easily obtained, based on the reported ZIKV cases from April 12th to August 24th (19 weeks) 2016 in Costa Rica, we apply the MCMC algorithm in Table 3 to estimate them. According to [3, 10], we fix the initial values of $\beta_1, \beta_2, \lambda_1$ and λ_2, with $\beta_1 = 0.207, \beta_2 = 0.125$ $\lambda_1 = 0.517$ and $\lambda_2 = 0.517$. We set the size M of mosquitos with $M = 2.1 \times 10^6$. It then follows that $\Theta(0) = (0.207, 0.125, 0.517, 0.517, 2.1 \times 10^6)$ in MCMC algorithm 3.

The initial conditions of model (4) are set as follows. Firstly, at the onset of ZIKV, we assume the initial value of the susceptible individuals $S(0)$ ($S^m(0)$+$S^f(0)$) to be 75% of the total size (4.757×10^6) of the population in Costa Rica at the beginning of 2016. For individuals of other states, we set $A(0) = I(0) \times \frac{q}{1-q}$ with $I(0) = 8$, which are the confirmed cumulative cases in initial stage, and $B(0) = J(0) = R(0) = 0$. The sex ratio is 1:1, so the initial values of male (female) individuals of all states are set as half of total numbers of each state, such as $S^{m(f)}(0) = S(0)/2$, $A^{m(f)}(0) = A(0)/2$ and $I^{m(f)}(0) = I(0)/2$. Then, we gave the initial values of males (females) with different degrees and states according to the degree distribution in Table 2, such as $S_k^{m(f)}(0) = S^{m(f)}(0) \times p_k^{m(f)}$ with $0 \le k \le 15$. Finally, for the mosquitoes population, since Costa Rica is a country where tourism is extremely popular, the initial infected cases may be imported by travellers from other infected countries and territories [35, 36, 37] and hence there are no or less infected mosquitos during the initial stage. Thus, we assume $M_i = 1$ and $M_s = M - 1 \approx M$.

Based on the initial conditions of parameters and variables of model (4) and degree distribution in Table 2, we run MCMC algorithm in Table 3 for 10000 iterations with a burn-in of 3000 iterations to estimate the parameters β_1, β_2, λ_1, λ_2 and M. Figure 5 show their empirical distributions, the corresponding mean values and the curves of the approximatively normal distributions. The specific values and range are displayed in Table 1.

3.2. The fitting results

According to the estimated parameters in Table 1 and degree distribution in Table 2, using MCMC in Table 3, Figure 6 illustrates a good fitting results of model (4) and the reported ZIKV cases from April 12th to August 24th 2016 in Costa Rica. The red solid curves show the median values of all 7000 simulations outputs and shaded region shows the 95% range. Figure 7 show the relative errors $(y - y^*)/y^*$ between theoretic and the reported data. All of them are below 20% and evenly distribute on both sides of the zero line, which suggests a good fit of the model to data.

3.3. The basic reproduction number

Mathematically, we apply the next generation matrix method developed by van den Driessche and Watmough [38] to calculate the basic reproduction number denoted by R_0 (see Appendix 6). The general form of R_0 is given in Appendix. Here, for explicit representation, we calculate two special cases for different parameter values.

Case 1. When $k_{max} = 0$ or $\beta_1 = \beta_2 = 0$, ZIKV is only transmitted by mosquitoes and the basic reproduction number of model (4) caused by mosquitoes is denoted by R_{hv} with

$$R_{hv} = \sqrt{\Big(\frac{q}{\gamma_1} + \frac{1-q}{\gamma_2}\Big)\frac{\lambda_1\lambda_2 M}{Nd}}. \tag{10}$$

In particular, when there are no asymptomatic infections, $q = 0$, the basic reproduction number R_{hv} reduces to

$$R^*_{hv} = \sqrt{\frac{\lambda_1\lambda_2 M}{\gamma_2 N d}},$$

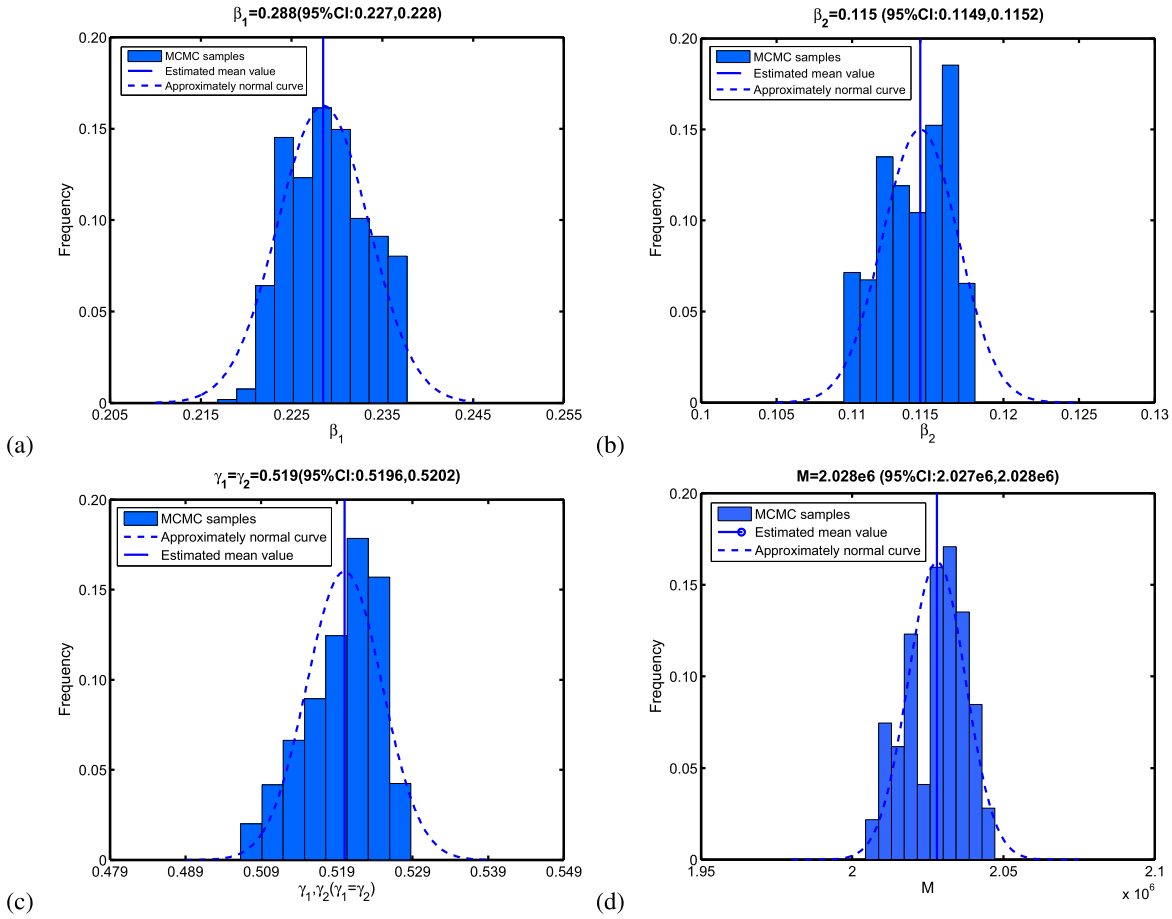

Figure 5: The estimation of model (4) parameters $\beta_1, \beta_2, \lambda_1, \lambda_2$ and M using MCMC. Subplot a, b, c and d show their empirical distributions, the corresponding mean values and the curves of the approximatively normal distributions.

which is consistent with the classical Ross-Macdonald malaria model [39].

Case 2. When $\lambda_1 = \lambda_2 = 0$ and $k_{max} \neq 0$. The basic reproduction number of model (4) caused only by the sexual transmission is denoted by R_{hh} with

$$R_{hh} = \sqrt{\Big(\frac{q}{\gamma_1} + \frac{1-q}{\gamma_2}\Big)\Big(\frac{q}{\gamma_1} + \frac{1-q}{\gamma_2} + \frac{q}{\mu_1} + \frac{1-q}{\mu_2}\Big)\beta_1\beta_2 \frac{\langle k^2\rangle_m}{\langle k\rangle_m}\frac{\langle k^2\rangle_f}{\langle k\rangle_f}}. \tag{11}$$

Particularly, when there are no asymptomatic infections, $q = 0$, the basic reproduction number reduces to

$$R^*_{hh} = \sqrt{\Big(\frac{1}{\gamma_2} + \frac{1}{\mu_2}\Big)\frac{\beta_1\beta_2}{\gamma_2}\frac{\langle k^2\rangle_m}{\langle k\rangle_m}\frac{\langle k^2\rangle_f}{\langle k\rangle_f}},$$

which coincides with the heterosexual transmission model [23].

Moreover, based on the values and the range of parameters in Table 1, the degree distribution of the overall network in Table 2 and the characteristic equation (16) in Appendix 6, we employ the Latin Hypercube Sampling (LHS) (see [40]) to generate 5000 samples by assuming a uniform distribution for each parameter to give the distribution of the basic reproduction number R_0 in Figure 8. The mean value of the basic reproduction number is $R_0 = 2.37$ (95%CI:

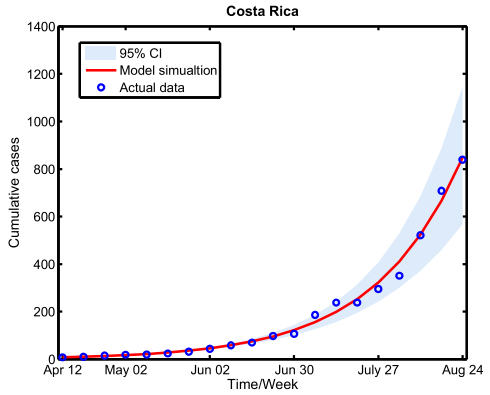

Figure 6: Fitting model (4) to data from April 12th to August 24th (19 weeks) 2016 in Costa Rica. Blue circles show the number of the reported cumulative cases, the shaded region show the 95% range of 7000 simulations, and the red curves is the median values of 7000 simulations.

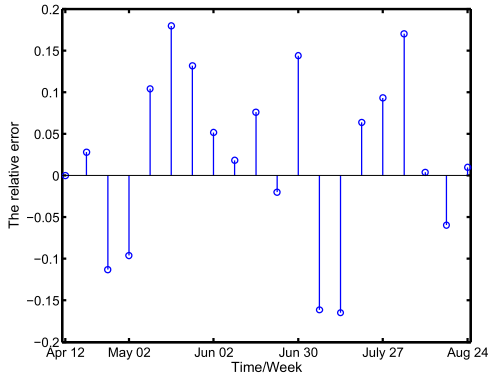

Figure 7: The relative errors between theoretical values of model (4) and the real data.

2.35,2.39), and mean values of R_{hv} (Eq. (10)) and R_{hh} (Eq. (11)) are $R_{hv} = 1.04$ (95%CI: 1.03,1.05) and $R_{hh} = 1.99$ (95%CI: 1.97,2.01), respectively. This indicates that sexual transmission has a larger effects on initiating an outbreak of ZIKV in Costa Rica than mosquito-human transmission. It may be because of the legalization of prostitution and unprotected sex activities in Cost Rica [41].

To determine the most sensitive parameters in R_0, we performed a sensitivity analysis via the partial rank correlation coefficients (PRCCs) for all input parameters against R_0 as shown in Figure 9, which illustrates the dependence of R_0 on each parameter. We choose a normal distribution with 5000 samples for all parameters with mean values in Table 1, and the respective standard deviations are 1×10^{-3} for β_1, 1×10^{-3} for β_2, 9×10^{-4} for λ_1, 6×10^{-3} for λ_2, 4×10^{-3} for γ_1, 4×10^{-3} for γ_2, 1×10^{-5} for μ_1, 1×10^{-5} for μ_2 and 2×10^{-5} for d. Figure 9 indicates that, the male-to-female transmission rate β_2, the female-to-male transmission rate β_1, the transmission rate λ_1 from an infected mosquito to a susceptible human, and the transmission rate λ_2 from an infected human to a susceptible mosquito are the most sensitive parameters in R_0. Figure 9 further shows that, the transfer rate γ_1, the natural birth and death rate d of mosquito, the transfer rate μ_1, and the transfer rate γ_2 reduce the spread of the disease. The parameters β_1 and β_2 are based on sexual transmission, λ_1 and λ_2 are based on mosquito-human transmission, but the PRCCs of them are very close. We conclude that both sexual and mosquito-human transmissions have a considerable effects on R_0 in Costa Rica, and that the effect of sexual transmission is slightly larger than that of mosquito-human transmission.

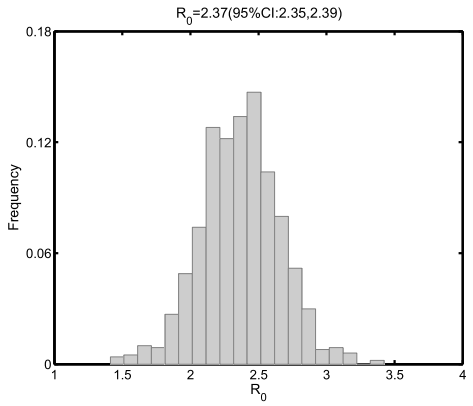

Figure 8: Distribution of the basic reproduction number R_0 in Costa Rica with mean $R_0 = 2.37$.

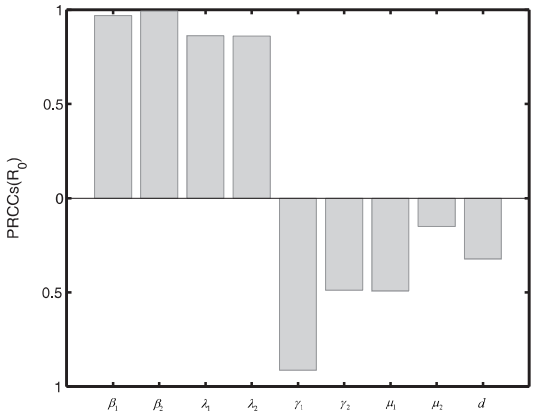

Figure 9: PRCCs illustrating the dependence of R_0 on each parameter.

In addition, we also find that the transfer rate γ_1 from state A to B, μ_1 from state B to R have a greater impact on R_0 than the transfer rate γ_2 from I to J, μ_2 from J to R at the same stage, respectively. In such cases, Figure 9 clearly suggest that, in order to effectively prevent ZIKV, the government should look for control measures to minimize the asymptomatic infected individuals.

To determine the dependence of R_0 on controllable parameters $\beta_1, \beta_2, \lambda_1$ and λ_2 of model (4), we take $\beta_1 = 0.228$ or in (0.220,0.235), $\beta_2 = 0.115$ or in (0.110,0.118) and let $\lambda = \lambda_1 = \lambda_2 = 0.519$ or in (0.510,0.528), and other parameters θ, q, γ_1, γ_2, μ_1, μ_2 and d take the corresponding values in Table 1. By fixing one of $\beta_1, \beta_2, \lambda$ and changing the other two parameters, Figure 10 represents the contour plots of R_0 with respect to λ and β_1, λ and β_2. It indicates that dampening both mosquito-human and sexual transmission simultaneously are effective measures to prevent ZIKV spread. For high-risk sexual transmission, controlling sexually active population at initial stage is an important and valid measure, which agrees with results in [3, 10].

In addition, the degree distribution of the network is a crucial factor in determining the basic reproduction number R_0, which generally depends on degree heterogeneity (mathematically, the moments of the degree distribution) [21]. To know the impact of degree heterogeneity on R_0, based on sex ratio 1:1 and the degree distribution in Table 2, we have $\langle k^2\rangle/\langle k\rangle = \langle k^2\rangle_m/\langle k\rangle_m = \langle k^2\rangle_f/\langle k\rangle_f$ as the measure of the heterogeneity level. Figure 11 shows the basic reproduction number R_0 against $\langle k^2\rangle/\langle k\rangle$ under three mean degrees, 1.4 (blue), 6 (red) and 10 (black). We can see that, R_0 increases whenever $\langle k^2\rangle/\langle k\rangle$ increases in the three cases, which correspond with the existing result of degree heterogeneity increasing epidemic threshold [21]. Therefore, an effective measure of controlling ZIKV infection at

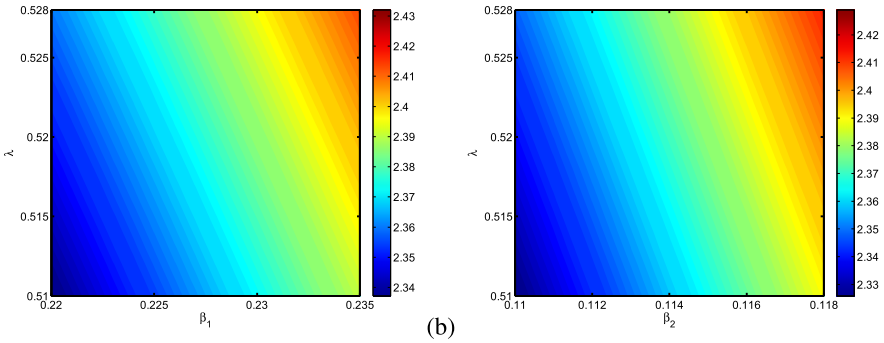

Figure 10: The contour map of the basic reproduction number R_0 with respect to controllable parameters: β_1 (the female-to-male transmission rate), β_2 (the male-to-female transmission rate) and λ (the transmission rate λ_1 (λ_2) from infected mosquito (human) to susceptible human (mosquito)) and $\lambda = \lambda_1 = \lambda_2$.

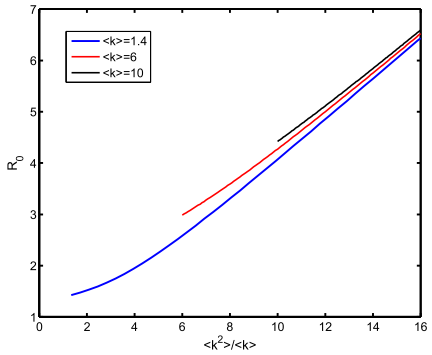

Figure 11: Dependence of R_0 on degree heterogeneity (characterized as $\langle k^2\rangle/\langle k\rangle$) for three mean degrees: 1.4 (blue), 6 (red) and 10 (black).

the onset is by supervising, isolating, quarantining and closing places with high-degree sex workers, and cutting off high-risk contacts so as to decrease the degree heterogeneity.

3.4. The epidemic final size

The final size is the proportion of the population experiencing infection (here including asymptomatic and symptomatic) during the epidemic, which is also an important characteristic parameter for epidemics of recovered individuals having permanent immune. Based on the parameters in Table 1, the final size is calculated as 48.33% that is near the reported final sizes of outbreaks on Yap Island in 2007 and French Polynesia in 2003-2014 [27]. Additionally, by the numerical solution, we calculate the contributions of the sexual and mosquitoes transmissions with 23.27% and 25.06%, respectively. It indicates that in the longer term, mosquitoes transmission has a slightly greater effect on the final size.

To further find the important factors that affect the final size, we carry out sensitivity analysis by PRCCs for all input parameters against the final size in Figure 12. The parameter values and standard deviations are the same as those for the basic reproduction number in Section 3.3. We can see that the final size is more sensitive to transmission rate λ_1 from infected mosquito to susceptible human than the transmission rate β_2 (β_1) from infected male (female) to susceptible female (male).

To determine the dependence of the final size on controllable parameters β_1, β_2, λ_1 and λ_2 of model (4), we take take $\beta_1 = 0.228$ or in (0.220,0.235), $\beta_2 = 0.115$ or in (0.110,0.118) and let $\lambda = \lambda_1 = \lambda_2 = 0.519$ or in (0.510,0.528),

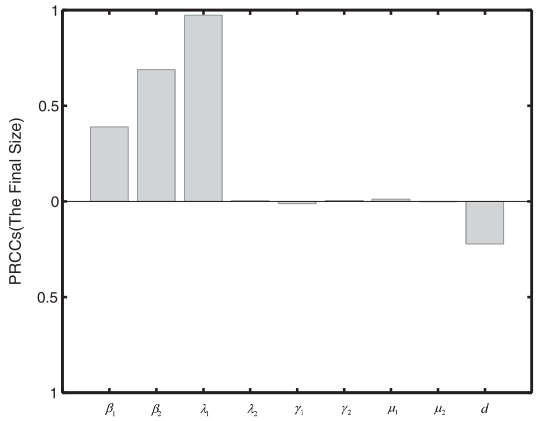

Figure 12: PRCCs illustrating the dependence of the final size on each parameter.

and other parameters θ, q, γ_1, γ_2, μ_1, μ_2 and d take the corresponding values in Table 1. By fixing one of β_1, β_2, λ and changing the other two parameters, Figure 13 shows the contour plots of the final size with respect to λ and β_1, λ and β_2. It implies that controlling both mosquito-human and sexual transmission are effective measures in decreasing the final size, but dampening the transmission rate λ between mosquitoes and humans is more effective, like spraying insect repellent on body. Nevertheless, we mainly consider the effects of sexual contacts on the course of ZIKV spread in the absence of control interventions for mosquito-human transmission.

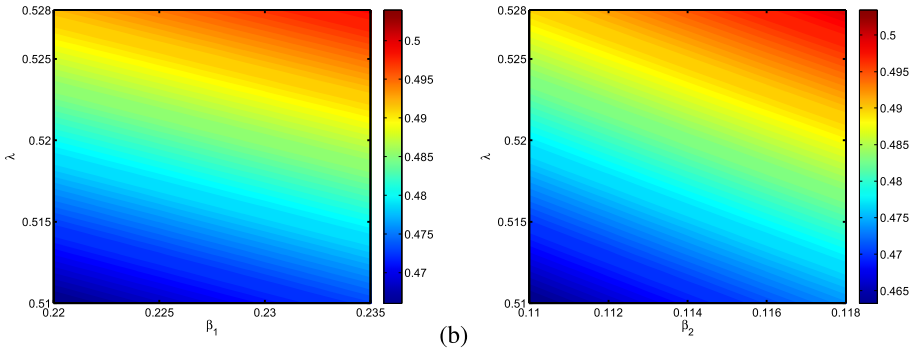

Figure 13: The contour map of the final size with respect to controllable parameters: β_1 (the female-to-male transmission rate), β_2 (the male-to-female transmission rate) and λ (the transmission rate λ_1 (λ_2) from infected mosquito (human) to susceptible human (mosquito)) and $\lambda = \lambda_1 = \lambda_2$.

3.5. The time threshold of taking intervention strategy

As indicated in [41], prostitution is legal in Costa Rica, sex workers within sexually active places, play a vital role in transmitting sexually transmitted infections (STIs). Intuitively, cutting off high-risk sexual contacts of individuals with large degree but small number (or changing degree heterogeneity) in the sexually active places may be an effective measure to prevent ZIKV spread, but the question is that when and how many of these can we isolate?

According to experienced observations in the Americas [3, 42], the proportions of females and males with more sexual contacts who are considered high risk are 0.07 and 0.09, respectively. Here, we take 0.0576 of the female population size and 0.0648 of the male population size as the high-risk individuals which precisely corresponds to the proportion of nodes with degree from 15 to 5 in the degree distribution in Table 2. Specifically, at a given time, we cut

off the contacts of these individuals by isolating the sexually active places and make them shift to the group of degree zero. The parameters of all the cases in model (4) are the same as those values in Table 1. The degree distribution after taking measures is modified to the distribution in Table 4, and the degree heterogeneity baseline $\langle k^2\rangle/\langle k\rangle$ changes from 5.63 to 1.67 for females and from 6.31 to 1.65 for males. The initial conditions of the groups with degree 1-4 and of mosquitoes after the measures keep the same as the corresponding final values before the measures, whereas the initial conditions of group with degree 0 are the sum of the corresponding final values of groups with degree 0 and groups with degree 5-15.

Table 4: The network degree distribution after cutting off contacts

Degree	0	1	2	3	4
Female Probability(p^f)	0.3676	0.4575	0.1057	0.0448	0.0244
Male Probability(p^m)	0.3748	0.4485	0.1064	0.0454	0.0249

Figure 14 (a) displays four cases of the cumulative cases (dashed lines) with the infected cases (solid lines) versus the time: case 1 without any other prevention and control measures (green), case 2 with cutting off contacts of individuals with degree 5-15 at week 19 (red), case 3 with cutting off contacts of individuals with degree 5-15 at week 45 (purple), and case 4 with cutting off contacts of individuals with degree 5-15 at week 71 (black). At week 19 and week 45 when we take cut-off measures or change the degree heterogeneity, Figure 14 (a) shows that the cumulative cases and final sizes are smaller than that in the case without any control measures. The 45th week corresponds to the peak time of the infected cases without control measures. However, at week 71, it shows that the cumulative case and final size are higher than that in the case without control measures (see inset in Figure 14 (a)). In detail, the steady cumulative case and the final size in the case without control measures are 3.104×10^5 and 48.33%, respectively. The steady cumulative cases in the three cases with control measures are 2.322×10^5, 2.939×10^5 and 3.119×10^5, respectively. The final sizes are 36.16%, 45.76% and 48.56%, respectively.

Inspired by Figure 14 (a), Figure 14 (b) illustrates the evolution of the final size with the time of taking measures. It indicates that there exists a threshold time 59.5, at which the cut-off measures keeps the final size unchanged, before which the measure decreases the final size (corresponding with purple and red curves in Figure 14 (a)), and after which the measure increases the final size (corresponding with black curve in Figure 14 (a)). In the case without mosquito-human transmission, the same phenomenon exists. Therefore, the reasons for this phenomenon may be rooted in nodes with large degrees but small number (only approximately 0.06 of the total population size) in the heterosexual networks. In the early of epidemic, once these nodes are infected they easily transmit disease to more neighbors than nodes with small-degree nodes. At this time, removing the contacts of these nodes by supervising, isolating, quarantining and closing the sexually active places help stem and delay the ZIKV spread (corresponding with the first two case). On the other hand, at the later stage of epidemic, these nodes are surrounded by more infected and recovered nodes, which forms clusters and further inhibits the spread of disease. At this stage, once these contacts from them are cut off, sexual activities among people with relatively low degrees will increase, which promotes ZIKV spread (corresponding with the third case).

To find the distribution of threshold time of cut-off sexual contacts of individuals with large degree (or changing degree heterogeneity) and peak time of infected cases, based on the parameter ranges and values in Table 1 and the same cut-off measure, we use LHS to generate 2000 samples by assuming a uniform distribution for each parameter to give the distribution of threshold time (red) and peak time (blue) in Figure 15. The two averages of threshold and peak times are calculated as 54.0 and 45.6. It follows that the cut-off measure is effective until threshold time.

The discovery of the threshold time provides a deadline for the authority to prevent ZIKV spread by closing sexually active place. The research indicates that the way of controlling ZIKV outbreak can be by changing the structure (degree distribution) of sexual-contact network, rather than only focusing on controlling mosquitoes in [16, 17, 18]. More attention should be paid to the monitor of the sexual transmission. It give us a guide of formulating control measure based on sexual transmission.

3.6. Disparity in the male/female cumulative and infected cases

For many sexually transmitted infections, the reported cases in males and females are discrepant and often higher in females. What has resulted in the phenomenon for ZIKA? Is it due to the different reported rates or the intrinsic

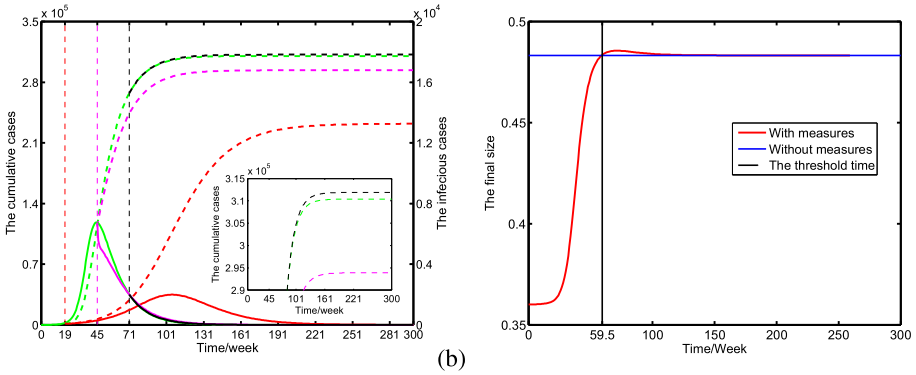

Figure 14: (a) The four cases of the cumulative cases (dashed line and left vertical scale) and infected cases (solid lines and right vertical scale) versus the time: the baseline case without any measures (green), the case of cutting off high risk contacts at week 19 (red), the case of cutting off high risk contacts at week 45 (purple) which is also the peak time of infected cases without measures and the case of cutting off high risk contacts at week 71 (black). (b) The final size without measure (blue solid line) and the final sizes with measures at each time (red solid line) based on the same parameters. The threshold time is week 59.5.

mechanism of these SITs? It is of great significance for the authorities to find out the essential causes to draw up the corresponding prevention and control measures. We give a clear and visual explanation on ZIKV infections in this section. Figure 16 illustrates the male/female cumulative and infected cases versus the time based on the parameters in Table 1. The inset shows the evolutions of the probability $\Theta^m(t)$ in Eq. (5) that any given contact of female individuals is linked to an infected male and the probability $\Theta^f(t)$ in Eq. (6) that any given contact of male individuals is linked to an infected female. We discover that the cumulative and infected cases in females are higher than in males, but the probability $\Theta^m(t)$ is bigger than the probability $\Theta^f(t)$. That is to say, sexually active females face larger sexually infected risk than sexually active males. Actually, from Eq. (5) and (6), we can see that the discovery is essentially because ZIKV exists in semen much longer than in blood and other body fluids [13], so different ZIKV cases in males and females are because of the intrinsic mechanism of ZIKV rather than the different reported rates. Compared with two ZIKV models in [10, 20], our model quantifies the sexually infected risk of females and males during the process of ZIKV infection via two network-based variables $\Theta^m(t)$ and $\Theta^f(t)$. It inspires us to focus more on the infected males when enacting control measures although the female cumulative and infected cases are higher.

4. Discussions and conclusions

The spread of ZIKV has caused global concern. Numerous researches focused on exploring the effects of mosquito-human transmission on ZIKV outbreak [16, 17, 18, 19] whereas only some works involved sexual transmission [3, 10, 20, 27]. In fact, due to the longer time of ZIKV in semen, sexual transmission plays an important role in ZIKV spread, especially for countries or regions with a high rate of sexually transmitted infections. More significantly, it is well known that network topological structure has a great impact on sexual transmission [22, 23, 43, 44]. However, there are few related works except that Saad-Roy [27] *et al.* applied an edge-based model to obtain the probability distribution of the time until the detection of microcephaly. In this paper, we took Costa Rica as a case study to develop a network-based model (4) of ZIKV spread via mean-field theory with mosquito-human and heterosexual transmissions, and further explored when and how changing the sexual network structure (the degree distribution) to control ZIKA spread in Costa Rica. In detail, the age factor was also considered by classifying humans in sexually inactive age as nodes of degree 0 and humans in sexually active age as nodes of degree more than 0. We estimated the degree distribution of sexually active individuals and all the individuals in Costa Rica according to demographic data in 2016. Compared with the influential well-mixed models on ZIKV such as Gao *et al.* 2016 [10], Maxian *et al.* 2017 [3], Agusto *et al.* 2017 [20] and so on, our model takes into account the heterogeneity of sexual contacts via the

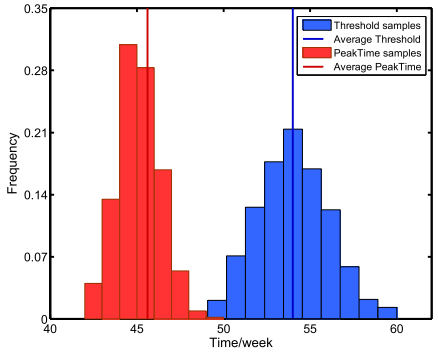

Figure 15: Distributions of cut-off threshold time (blue) and peak time (red) of infected cases without measures with average threshold=54.0 (blue line) and peak time=45.6 (red line).

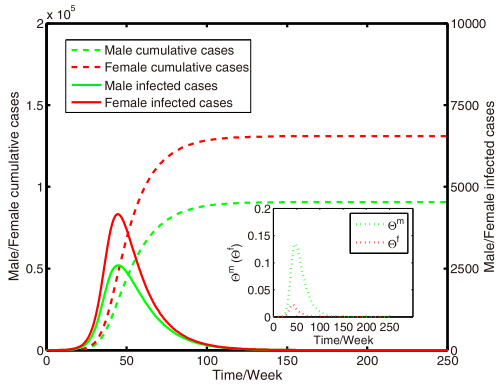

Figure 16: The male (green)/female (red) cumulative (dashed line and left vertical scale) and infected (solid lines and right vertical scale) cases based on the parameters in Table 1. The inset shows the evolution of the probability $\Theta^m(t)$—green and dot-dash line ($\Theta^f(t)$—red and dot-dash line) in Eq. (5) and (6).

degree distribution based on the demographic data of Costa Rica 2016, which includes more detailed information of individual interactions—crucial in understanding ZIKV sexual transmission deeply.

Based on the estimated degree distribution and limited data of cumulative cases of ZIKA, a good fitting results for model (4) (Figure 6) were obtained. Under the assumption of constant mosquito size, the basic reproduction number was estimated as $R_0 = 2.37$ (95%CI: 2.35,2.39) with $R_{hv} = 1.04$ (95%CI: 1.03,1.05) and $R_{hh} = 1.99$ (95%CI: 1.97,2.01). Both the basic reproduction number R_{hh} without human-mosquito transmission and the basic reproduction number R_{hv} without human-human transmission are more than one. In other words, either sexual transmission or human-mosquito transmission may initiate an outbreak of ZIKV in Costa Rica, which is different from the result in Brazil that only human-mosquito transmission may initiate an outbreak [3, 10]. In addition, the final size (the proportion of the population experiencing infection during the epidemic) was estimated as 48.33% with contribution of 23.27% by sexual transmission and 25.06% by mosquito-human transmission, respectively. It can be seen that sexual transmission has a large contribution to the basic reproduction number and the final size. The possible reason is that Costa Rica is a country where prostitution is legal and regulated [41]. In order to make our results more convincing, we did the simulation based on model and parameter setting of Gao *et al* 2016 [10]. If β is assumed as 0.2 (instead of 0.05, which is a low estimate by Gao *et al.*), we perform random selection of parameters in the same ranges as Gao *et al.* for β in 0.01 to 0.4. The R_{hh} (which is the R_0 component for human to human transmission, mainly through sexual contacts) can be as high as 3. The attack rate (equal to the final size for emergent SIR epidemic) of

human to human transmission (sexual transmission) can be as high as 40% of the population, which is very high. Even if only 20% of the population is already very high. The simulation to Gao *et al.* 2016 [10] indicates that the sexual transmission in some special cases (countries like Costa Rica) could be very substantial, which agrees with our result. Thus, more attention should be also paid to sexual transmission not just mosquito-human transmission when making the prevention and control measures on ZIKV, especially in counties with high rate of sexually transmitted infections, which is also demonstrated by our sensitivity analysis (Figure 9) on R_0 and (Figure 12) on the final size.

From the viewpoint of network topological structure, we take $\langle k^2\rangle/\langle k\rangle$ as the baseline to measure degree heterogeneity. Figure 11 shows that R_0 increases with the increase in $\langle k^2\rangle/\langle k\rangle$, which indicates that large degree heterogeneity results in greater R_0. Thus, cutting off the high-risk contacts by supervising, isolating, quarantining and closing places with high-degree sexual partners to lower degree heterogeneity, is an efficient measure to suppress ZIKV dissemination at the onset of the epidemic. Intuitively, when ZIKV begins to disseminate, we also take the same cut-off measures to inhibit ZIKV infection and lower the final size. Figure 14(a) shows the processes of ZIKV infection at three different times of taking the measure: the 19th, 45th and 71th weeks. It is surprisingly found that compared with the case without any measures (green curves in Figure 14 (a)), except for the intuitive decrease in cumulative cases and the final sizes (19th week, red curves and 45th week, purple curves in Figure 14 (a)), there exists an increase case (71th week, black curves in Figure 14 (a)). Figure 14 (b) illustrates the threshold time of taking measures. Although it is well known that scale-free network is vulnerable to attack on the nodes with high degree and centrality, we find that when attacking the same proportion of nodes with high degree and centrality in these networks at different time, the epidemic final size has a great difference. As Figure 14 (a) and (b) indicated, cutting off high-risk sexual contacts of individuals with large degree in the sexually active places is a double-edged sword, either restraining or boosting the ZIKV spread, which depends on the time of taking the measures. By using LHS we obtained the distribution of the threshold time of taking measures and peak time of infected cases (Figure 15) and the mean threshold, peak times are 54.0, 45.6, respectively. Consequently, it may be valid to cut off high-risk contacts until the threshold time, which provides a good guide for the government to prevent ZIKV spread from the viewpoint of control sexual-contact network structure.

Additionally, it is helpful for the government to get deep insight into the evolution of the cumulative and infected cases of ZIKV in males and females with time, and especially the discrepant sexually infected risks of the males and females. Via two edge-based probabilities $\Theta^m(t)$ (Eq. (5)), $\Theta^f(t)$ (Eq. (6)) that any given contact of female, male individuals is linked to an infected male, female individual, compared with two ZIKV models in [10, 20], our model provides a quantitative result about the sexually infected risks the males and females face (see Figure 16). From Figure 16, we can see that $\Theta^m(t)$ is bigger than $\Theta^f(t)$ at a given time t(see inset in Figure 16), although the cumulative and infected cases in females are higher than those in males. It indicates that females face greater infection risk from infected males since ZIKV exists in semen for a longer time, which reminds us that we should pay more attention to infected males.

We propose a possible explanation/scenario and control schemes for high sex-transmission-induced infected cases in those countries where prostitution is legal. More surveillance data with the type of route of transmission information would be necessary to confirm our hypothesis. Nevertheless, the methodology of the model is novel and potentially useful for mitigation planning. In countries where prostitution is legal, the monitor of the sexual transmission should be enhanced. Our model can be applicable to other countries, which depends on the degree distribution, the parameters and the initial values of model variables of the given country. When the mosquito is prevalent (or less prevalent), the parameters and size related to mosquitoes is big (or small). When sexual activity is active (or inactive), the parameters and size related to sexual transmission is big (or small), and the degree distribution needs to reset based on the settings of the given country. In addition, the mosquitoes distribution across regions due to elevation, rainfall and topography, and other topological properties of sexual contact network like clustering and community have impacts of great importance on ZIKV spread. Future models should include those factors, which need more corresponding data.

5. Acknowledgements

We thank Professor Rui Xu, Juan Zhang and colleague Asamoah Kiddy K. Joshua in our lab and Xianghong Zhang in York University for useful discussions and suggestions. We also thank the reviewers and editors for their comments and suggestions. This work was supported by the National Natural Science Foundation of China (61873154, 11701348, 11671241,11571210), Shanxi Key Laboratory (201705D111006), National Key Research and

Development Program of China (2016YFD05 01500),GraduateStudents Excellent Innovative Item of Shanxi Province (2017BY003), Shanxi Scientific and Technology Innovation Team (201805D131012-1) and the Youth Science Fund of Shanxi Province (2015021020).

6. Appendix—The calculation of the basic reproduction number of model (4)

Obviously, the disease-free equilibrium of model (4) is

$$E_0 = \Big(\underbrace{N_0^m, 0, 0, 0, 0, 0, N_0^f, 0, 0, 0}, \underbrace{N_1^m, 0, 0, 0, 0, 0, N_1^f, 0, 0, 0}, \cdots, \underbrace{N_{k_{max}}^m, 0, 0, 0, 0, 0, N_{k_{max}}^f, 0, 0, 0}, M, 0\Big).$$

For notation clarity, according to (2), let $G = \sum_l lN_l^m = \sum_l lN_l^f$. Note that only compartments A_k^m, I_k^m, B_k^m, J_k^m, A_k^f, I_k^f and M_i are involved in the calculation of the basic reproduction number. Thus, at the disease-free state E_0, the rate F of appearance of new infections and the rate V of transfer of individuals out of the compartment are given by

$$F = \begin{pmatrix} F_{00} & F_{01} & F_{02} & \cdots & F_{0k_{max}} & F_{0(k_{max}+1)} \\ F_{10} & F_{11} & F_{12} & \cdots & F_{1k_{max}} & F_{1(k_{max}+1)} \\ F_{20} & F_{21} & F_{22} & \cdots & F_{2k_{max}} & F_{2(k_{max}+1)} \\ \vdots & \vdots & \vdots & \ddots & \vdots & \vdots \\ F_{k_{max}0} & F_{k_{max}1} & F_{k_{max}2} & \cdots & F_{k_{max}k_{max}} & F_{k_{max}(k_{max}+1)} \\ F_{(k_{max}+1)0} & F_{(k_{max}+1)1} & F_{(k_{max}+1)2} & \cdots & F_{(k_{max}+1)k_{max}} & 0 \end{pmatrix}_{6(k_{max}+1)+1}, \tag{12}$$

where

$$F_{ij} = \begin{pmatrix} 0 & 0 & 0 & 0 & \frac{q\beta_2}{G} ijN_j^f & \frac{(1-q)\beta_2}{G} ijN_j^f \\ 0 & 0 & 0 & 0 & \frac{q\beta_2}{G} ijN_j^f & \frac{(1-q)\beta_2}{G} ijN_j^f \\ 0 & 0 & 0 & 0 & \frac{q\beta_2}{G} ijN_j^f & \frac{(1-q)\beta_2}{G} ijN_j^f \\ 0 & 0 & 0 & 0 & \frac{q\beta_2}{G} ijN_j^f & \frac{(1-q)\beta_2}{G} ijN_j^f \\ \frac{q\beta_1}{G} ijN_j^m & \frac{(1-q)\beta_1}{G} ijN_j^m & 0 & 0 & 0 & 0 \\ \frac{q\beta_1}{G} ijN_j^m & \frac{(1-q)\beta_1}{G} ijN_j^m & 0 & 0 & 0 & 0 \end{pmatrix},$$

$$F_{i(k_{max}+1)} = \left(\frac{\lambda_2 M}{N}, \frac{\lambda_2 M}{N}, 0, 0, \frac{\lambda_2 M}{N}, \frac{\lambda_2 M}{N}\right)^T,$$

$$F_{(k_{max}+1)j} = \left(\frac{q\lambda_1}{N} N_j^m, \frac{(1-q)\lambda_1}{N} N_j^m, 0, 0, \frac{q\lambda_1}{N} N_j^f, \frac{(1-q)\lambda_1}{N} N_j^f\right), \quad i, j = 0, 1, 2, \cdots, k_{max},$$

and

$$V = \begin{pmatrix} V_{00} & & & & & \\ & V_{11} & & & & \\ & & V_{22} & & & \\ & & & \ddots & & \\ & & & & V_{k_{max}k_{max}} & \\ & & & & & d \end{pmatrix}_{6(k_{max}+1)+1}, \tag{13}$$

where

$$V_{ii} = \begin{pmatrix} \gamma_1 & 0 & -\gamma_1 & 0 & 0 & 0 \\ & \gamma_2 & 0 & -\gamma_2 & 0 & 0 \\ & & \mu_1 & 0 & 0 & 0 \\ & & & \mu_2 & 0 & 0 \\ & & & & \gamma_1 & 0 \\ & & & & & \gamma_2 \end{pmatrix}, \quad i = 0, 1, 2, \cdots, k_{max}.$$

It follows that

$$FV^{-1} =$$
$$\left(\begin{array}{cccccc}
F_{00}V_{00}^{-1} & F_{01}V_{11}^{-1} & F_{02}V_{22}^{-1} & \cdots & F_{0k_{max}}V_{k_{max}k_{max}}^{-1} & F_{0(k_{max}+1)}V_{(k_{max}+1)(k_{max}+1)}^{-1} \\
F_{10}V_{00}^{-1} & F_{11}V_{11}^{-1} & F_{12}V_{22}^{-1} & \cdots & F_{1k_{max}}V_{k_{max}k_{max}}^{-1} & F_{1(k_{max}+1)}V_{(k_{max}+1)(k_{max}+1)}^{-1} \\
F_{20}V_{00}^{-1} & F_{21}V_{11}^{-1} & F_{22}V_{22}^{-1} & \cdots & F_{2k_{max}}V_{k_{max}k_{max}}^{-1} & F_{2(k_{max}+1)}V_{(k_{max}+1)(k_{max}+1)}^{-1} \\
\vdots & \vdots & \vdots & \ddots & \vdots & \vdots \\
F_{k_{max}0}V_{00}^{-1} & F_{k_{max}1}V_{11}^{-1} & F_{k_{max}2}V_{22}^{-1} & \cdots & F_{k_{max}k_{max}}V_{k_{max}k_{max}}^{-1} & F_{k_{max}(k_{max}+1)}V_{(k_{max}+1)(k_{max}+1)}^{-1} \\
F_{(k_{max}+1)0}V_{00}^{-1} & F_{(k_{max}+1)1}V_{11}^{-1} & F_{(k_{max}+1)2}V_{22}^{-1} & \cdots & F_{(k_{max}+1)k_{max}}V_{k_{max}k_{max}}^{-1} & 0
\end{array}\right) \tag{14}$$

where

$$F_{ij}V_{jj}^{-1} = \left(\begin{array}{cccccc}
0 & 0 & 0 & 0 & \frac{q\beta_2}{\gamma_1 G} ijN_j^f & \frac{(1-q)\beta_2}{\gamma_2 G} ijN_j^f \\
0 & 0 & 0 & 0 & \frac{q\beta_2}{\gamma_1 G} ijN_j^f & \frac{(1-q)\beta_2}{\gamma_2 G} ijN_j^f \\
0 & 0 & 0 & 0 & \frac{q\beta_2}{\gamma_1 G} ijN_j^f & \frac{(1-q)\beta_2}{\gamma_2 G} ijN_j^f \\
0 & 0 & 0 & 0 & \frac{q\beta_2}{\gamma_1 G} ijN_j^f & \frac{(1-q)\beta_2}{\gamma_2 G} ijN_j^f \\
\frac{q\beta_1}{\gamma_1 G} ijN_j^m & \frac{(1-q)\beta_1}{\gamma_2 G} ijN_j^m & \frac{q\beta_1}{\mu_1 G} ijN_j^m & \frac{(1-q)\beta_1}{\mu_2 G} ijN_j^m & 0 & 0 \\
\frac{q\beta_1}{\gamma_1 G} ijN_j^m & \frac{(1-q)\beta_1}{\gamma_2 G} ijN_j^m & \frac{q\beta_1}{\mu_1 G} ijN_j^m & \frac{(1-q)\beta_1}{\mu_2 G} ijN_j^m & 0 & 0
\end{array}\right),$$

$$F_{i(k_{max}+1)}V_{(k_{max}+1)(k_{max}+1)}^{-1} = \left(\frac{\lambda_2 M}{Nd}, \frac{\lambda_2 M}{Nd}, 0, 0, \frac{\lambda_2 M}{Nd}, \frac{\lambda_2 M}{Nd}\right)^T,$$

$$F_{(k_{max}+1)j}V_{jj}^{-1} = \left(\frac{q\lambda_1}{\gamma_1 N}N_j^m, \frac{(1-q)\lambda_1}{\gamma_2 N}N_j^m, \frac{q\lambda_1}{\mu_1 N}N_j^m, \frac{(1-q)\lambda_1}{\mu_2 N}N_j^m, \frac{q\lambda_1}{\gamma_1 N}N_j^f, \frac{(1-q)\lambda_1}{\gamma_2 N}N_j^f\right), \quad i, j = 0, 1, 2, \cdots, k_{max}.$$

Referring to [38], the basic reproduction number is defined as the spectral radius of the matrix FV^{-1} and the spectral radius is the leading eigenvalue of FV^{-1}. Thus, we need to solve the leading eigenvalue of FV^{-1}. We perform a series of similarity transformations on the matrix FV^{-1}, and the resulting similar matrix is

$$\left(\begin{array}{cc} F_{11}^* & F_{12}^* \\ F_{21}^* & F_{22}^* \end{array}\right)_{6k_{max}+1},$$

where

$$F_{11}^* = \left(\begin{array}{cccc}
0 & 0 & 0 & \frac{\lambda_2 M}{Nd} \\
(\frac{q}{\gamma_1} + \frac{1-q}{\gamma_2})\beta_2 & 0 & (\frac{q}{\gamma_1} + \frac{1-q}{\gamma_2})\beta_2 \frac{\langle k^2\rangle_f}{\langle k\rangle_f} & 0 \\
(\frac{q}{\gamma_1} + \frac{1-q}{\gamma_2})\beta_1 & (\frac{q}{\gamma_1} + \frac{1-q}{\gamma_2} + \frac{q}{\mu_1} + \frac{1-q}{\mu_2})\beta_1 \frac{\langle k^2\rangle_m}{\langle k\rangle_m} & 0 & 0 \\
(\frac{q}{\gamma_1} + \frac{1-q}{\gamma_2})\lambda_1 & (\frac{q}{\gamma_1} + \frac{1-q}{\gamma_2} + \frac{q}{\mu_1} + \frac{1-q}{\mu_2})\lambda_1 \langle k\rangle_m & (\frac{q}{\gamma_1} + \frac{1-q}{\gamma_2})\lambda_1 \langle k\rangle_f & 0
\end{array}\right), \tag{15}$$

$$F_{21}^* = 0_{(6(k_{max}+1)-3)\times 4}, \quad \text{and} \quad F_{22}^* = 0_{(6(k_{max}+1)-3)\times(6(k_{max}+1)-3)}.$$

Obviously, FV^{-1} in Eq. (14) and F_{11}^* in Eq. (15) have the same leading eigenvalue. Additionally, since F_{11}^* is non negative, according to the Perron-Frobenius theorem it has a single, unique eigenvalue as the basic reproduction number denoted by R_0 which is positive, real, and strictly greater than all the others. The characteristic equation of F_{11}^* is

$$\lambda^4 + a_2\lambda^2 + a_1\lambda + a_0 = 0, \tag{16}$$

where

$$\begin{aligned}
a_2 &= -\left(\frac{q}{\gamma_1} + \frac{1-q}{\gamma_2}\right)\frac{\lambda_1\lambda_2 M}{Nd} - \left(\frac{q}{\gamma_1} + \frac{1-q}{\gamma_2}\right)\left(\frac{q}{\gamma_1} + \frac{1-q}{\gamma_2} + \frac{q}{\mu_1} + \frac{1-q}{\mu_2}\right)\beta_1\beta_2\frac{\langle k^2\rangle_m\langle k^2\rangle_f}{\langle k\rangle_m\langle k\rangle_f} < 0, \\
a_1 &= -\frac{\lambda_1\lambda_2 M}{Nd}\left(\frac{q}{\gamma_1} + \frac{1-q}{\gamma_2}\right)\left[\beta_2\langle k\rangle_m\left(\frac{q}{\gamma_1} + \frac{1-q}{\gamma_2} + \frac{q}{\mu_1} + \frac{1-q}{\mu_2}\right) + \beta_1\langle k\rangle_f\left(\frac{q}{\gamma_1} + \frac{1-q}{\gamma_2}\right)\right] < 0, \\
a_0 &= \left(\frac{q}{\gamma_1} + \frac{1-q}{\gamma_2}\right)^2\left(\frac{q}{\gamma_1} + \frac{1-q}{\gamma_2} + \frac{q}{\mu_1} + \frac{1-q}{\mu_2}\right)\frac{\lambda_1\lambda_2\beta_1\beta_2 M}{Nd}\left(\frac{\langle k^2\rangle_m\langle k^2\rangle_f}{\langle k\rangle_m\langle k\rangle_f} - \frac{\langle k^2\rangle_m\langle k\rangle_f}{\langle k\rangle_m} - \frac{\langle k^2\rangle_f\langle k\rangle_m}{\langle k\rangle_f}\right).
\end{aligned}$$

Based on the characteristic equation (16), the basic reproduction number can be obtained numerically in Section 3.3. In what follows, we give the general solutions according to the following Lemma 6.1 and Ferrari's solution [45].

Lemma 6.1. *Consider the general cubic equation[46]:*

$$\tilde{a}x^3 + \tilde{b}x^2 + \tilde{c}x + \tilde{d} = 0, \tag{17}$$

where $\tilde{a}, \tilde{b}, \tilde{c}, \tilde{d} \in \mathrm{R}$ *and* $\tilde{a} \neq 0$*. Denote*

$$A = \tilde{b}^2 - 3\tilde{a}\tilde{c}, B = \tilde{b}\tilde{c} - 9\tilde{a}\tilde{d}, C = \tilde{c}^2 - 3\tilde{b}\tilde{d}, \Delta = B^2 - 4AC,$$

then we have the following results:

1. *When* $A = B = 0$*, Eq.* (17) *has a triple root;*
2. *When* $\Delta > 0$*, Eq.* (17) *has one real root and one pair of conjugate virtual roots;*
3. *When* $\Delta = 0$*, Eq.* (17) *has three real roots and two of which are repeated roots;*
4. *When* $\Delta < 0$*, Eq.* (17) *has three different real roots.*

In order to obtain the exact solution of Eq. (16), we use the Ferrari's solution with the same notation as [45]. let $\tilde{p} = a_2, \tilde{q} = a_1, \tilde{r} = a_0$ and then we can get the equation with respect to an introduced variable $\tilde{m}$

$$8\tilde{m}^3 + 8a_2\tilde{m}^2 + 2(a_2^2 - 4a_0)\tilde{m} - a_1^2 = 0.$$

In order to find $\tilde{m}$, we solve the cubic equation according to Lemma 6.1. Let $\tilde{a} = 8, \tilde{b} = 8a_2, \tilde{c} = 2(a_2^2 - 4a_0), \tilde{d} = -a_1^2$ and then

$$\begin{aligned}
A &= \tilde{b}^2 - 3\tilde{a}\tilde{c} = 16(a_2^2 + 12a_0) = 16(R_{hv}^2 + R_{hh}^2)^2 + 192R_{hv}^2R_{hh}^2\left(1 - \frac{\langle k\rangle_f^2}{\langle k^2\rangle_f} - \frac{\langle k\rangle_m^2}{\langle k^2\rangle_m}\right),\\
B &= \tilde{b}\tilde{c} - 9\tilde{a}\tilde{d} = 64a_2(a_2^2 - 4a_0) + 72a_1^2\\
&= -64(R_{hv}^2 + R_{hh}^2)\left[(R_{hv}^2 + R_{hh}^2)^2 - 4R_{hv}^2R_{hh}^2\left(1 - \frac{\langle k\rangle_f^2}{\langle k^2\rangle_f} - \frac{\langle k\rangle_m^2}{\langle k^2\rangle_m}\right)\right]\\
&+72R_{hv}^4\left(\beta_2\langle k\rangle_m(\frac{q}{\gamma_1} + \frac{1-q}{\gamma_2} + \frac{q}{\mu_1} + \frac{1-q}{\mu_2}) + \beta_1\langle k\rangle_f(\frac{q}{\gamma_1} + \frac{1-q}{\gamma_2})\right)^2,\\
C &= \tilde{c}^2 - 3\tilde{b}\tilde{d} = 4(a_2^2 - 4a_0)^2 + 24a_1^2a_2,\\
&= 4\left[(R_{hv}^2 + R_{hh}^2)^2 - 4R_{hv}^2R_{hh}^2\left(1 - \frac{\langle k\rangle_f^2}{\langle k^2\rangle_f} - \frac{\langle k\rangle_m^2}{\langle k^2\rangle_m}\right)\right]^2\\
&-24(R_{hv}^2 + R_{hh}^2)R_{hv}^4\left(\beta_2\langle k\rangle_m(\frac{q}{\gamma_1} + \frac{1-q}{\gamma_2} + \frac{q}{\mu_1} + \frac{1-q}{\mu_2}) + \beta_1\langle k\rangle_f(\frac{q}{\gamma_1} + \frac{1-q}{\gamma_2})\right)^2,\\
\Delta &= B^2 - 4AC.
\end{aligned}$$

Further, we consider the following four cases:

Case 1. When $A = B = 0$, we choose $\tilde{m} = \frac{-\tilde{b}}{3\tilde{a}} = -\frac{a_2}{3} = \frac{1}{3}(R_{hv}^2 + R_{hh}^2)$;

Case 2. When $\Delta > 0$, we choose $\tilde{m} = \frac{-\tilde{b} - \sqrt[3]{Y_1} - \sqrt[3]{Y_2}}{3\tilde{a}} = \frac{-8a_2 - \sqrt[3]{Y_1} - \sqrt[3]{Y_2}}{24} = \frac{8(R_{hv}^2 + R_{hh}^2) - \sqrt[3]{Y_1} - \sqrt[3]{Y_2}}{24}$,
$Y_{1,2} = A\tilde{b} + 3\tilde{a}(\frac{-B \pm \sqrt{B^2 - 4AC}}{2}) = 8a_2A + 12(-B \pm \sqrt{\Delta}) = -8(R_{hv}^2 + R_{hh}^2)A + 12(-B \pm \Delta)$;

Case 3. When $\Delta = 0$, we choose $\tilde{m} = -\frac{B}{2A}$;

Case 4. When $\Delta < 0$, we choose $\tilde{m} = \frac{-\tilde{b} - 2\sqrt{A}cos\frac{\theta}{3}}{3\tilde{a}} = \frac{-8a_2 - 2\sqrt{A}cos\frac{\theta}{3}}{24} = \frac{8(R_{hv}^2 + R_{hh}^2) - 2\sqrt{A}cos\frac{\theta}{3}}{24}, \theta = \arccos T$,
$T = \frac{2A\tilde{b} - 3\tilde{a}B}{2\sqrt{A^3}} = \frac{16a_2A - 24B}{2\sqrt{A^3}} = \frac{-16(R_{hv}^2 + R_{hh}^2)A - 24B}{2\sqrt{A^3}}, A > 0, -1 < T < 1$.

For each case, we can obtain $\tilde{m}$, then the roots of Eq. (16) are listed as follows:

$$\begin{aligned}
\lambda_1 &= \frac{-\sqrt{2\tilde{m}} + \sqrt{-\left(2\tilde{p} + 2\tilde{m} - \frac{\sqrt{2}\tilde{q}}{\sqrt{\tilde{m}}}\right)}}{2} = \frac{-\sqrt{2\tilde{m}} + \sqrt{-\left(2a_2 + 2\tilde{m} - \frac{\sqrt{2}a_1}{\sqrt{\tilde{m}}}\right)}}{2}\\
&= \frac{1}{2}\left(-\sqrt{2\tilde{m}} + \sqrt{-\left(-2(R_{hv}^2 + R_{hh}^2) + 2\tilde{m} + \frac{\sqrt{2}}{\sqrt{\tilde{m}}}R_{hv}^2\left(\beta_2\langle k\rangle_m(\frac{q}{\gamma_1} + \frac{1-q}{\gamma_2} + \frac{q}{\mu_1} + \frac{1-q}{\mu_2}) + \beta_1\langle k\rangle_f(\frac{q}{\gamma_1} + \frac{1-q}{\gamma_2})\right)\right)}\right),
\end{aligned}$$

$$
\begin{aligned}
\lambda_2 &= \frac{-\sqrt{2\tilde{m}}-\sqrt{-\left(2\tilde{p}+2\tilde{m}-\frac{\sqrt{2}\tilde{q}}{\sqrt{\tilde{m}}}\right)}}{2} = \frac{-\sqrt{2\tilde{m}}-\sqrt{-\left(2a_2+2\tilde{m}-\frac{\sqrt{2}a_1}{\sqrt{\tilde{m}}}\right)}}{2} \\
&= \frac{1}{2}\left(-\sqrt{2\tilde{m}}-\sqrt{-\left(-2(R_{hv}^2+R_{hh}^2)+2\tilde{m}+\frac{\sqrt{2}}{\sqrt{\tilde{m}}}R_{hv}^2\left(\beta_2\langle k\rangle_m(\frac{q}{\gamma_1}+\frac{1-q}{\gamma_2}+\frac{q}{\mu_1}+\frac{1-q}{\mu_2})+\beta_1\langle k\rangle_f(\frac{q}{\gamma_1}+\frac{1-q}{\gamma_2})\right)\right)}\right), \\
\lambda_3 &= \frac{\sqrt{2\tilde{m}}+\sqrt{-\left(2\tilde{p}+2\tilde{m}+\frac{\sqrt{2}\tilde{q}}{\sqrt{\tilde{m}}}\right)}}{2} = \frac{\sqrt{2\tilde{m}}+\sqrt{-\left(2a_2+2\tilde{m}+\frac{\sqrt{2}a_1}{\sqrt{\tilde{m}}}\right)}}{2}, \qquad (18) \\
&= \frac{1}{2}\left(\sqrt{2\tilde{m}}+\sqrt{-\left(-2(R_{hv}^2+R_{hh}^2)+2\tilde{m}-\frac{\sqrt{2}}{\sqrt{\tilde{m}}}R_{hv}^2\left(\beta_2\langle k\rangle_m(\frac{q}{\gamma_1}+\frac{1-q}{\gamma_2}+\frac{q}{\mu_1}+\frac{1-q}{\mu_2})+\beta_1\langle k\rangle_f(\frac{q}{\gamma_1}+\frac{1-q}{\gamma_2})\right)\right)}\right), \\
\lambda_4 &= \frac{\sqrt{2\tilde{m}}-\sqrt{-\left(2\tilde{p}+2\tilde{m}+\frac{\sqrt{2}\tilde{q}}{\sqrt{\tilde{m}}}\right)}}{2} = \frac{\sqrt{2\tilde{m}}-\sqrt{-\left(2a_2+2\tilde{m}+\frac{\sqrt{2}a_1}{\sqrt{\tilde{m}}}\right)}}{2} \\
&= \frac{1}{2}\left(\sqrt{2\tilde{m}}-\sqrt{-\left(-2(R_{hv}^2+R_{hh}^2)+2\tilde{m}-\frac{\sqrt{2}}{\sqrt{\tilde{m}}}R_{hv}^2\left(\beta_2\langle k\rangle_m(\frac{q}{\gamma_1}+\frac{1-q}{\gamma_2}+\frac{q}{\mu_1}+\frac{1-q}{\mu_2})+\beta_1\langle k\rangle_f(\frac{q}{\gamma_1}+\frac{1-q}{\gamma_2})\right)\right)}\right).
\end{aligned}
$$

Because of nonnegativity of F_{11}^*, the unique, positive and real eigenvalue with the largest modulus among λ_1, λ_2, λ_3 and λ_4 is the basic reproduction number R_0.

[1] Campos GS, Bandeira AC, Sardi, SI. 2015 Zika virus outbreak, Bahia, Brazil. Emerg. Infect. Dis. **21**(10), 1885. (doi: 10.3201/eid2110.150847)

[2] Foy, BD, Kobylinski KC, Chilson Foy JL, Blitvich BJ, Travassos DRA, Haddow AD, Lanciotti RS, Tesh RB. 2011 Probable non-vector-borne transmission of Zika virus, Colorado, USA. Emerg. Infect. Dis. **17**(5), 880. (doi: 10.3201/eid1705.101939)

[3] Maxian O, Neufeld A, Talis EJ, Childs LM, Blackwood JC. 2017 Zika virus dynamics: when does sexual transmission matter?. Epidemics **21**(C). (doi: 10.1016/j.epidem.2017.06.003)

[4] Aubry M, Teissier A, Huart M, Merceron S, Vanhomwegen J, Roche C, Vial AL, Teururai S, Sicard S, Paulous S. 2017 Zika Virus Seroprevalence, French Polynesia, 2014-2015. Emerg. Infect. Dis. **23**(4), 669. (doi: 10.3201/eid2304.161549)

[5] Rasmussen SA, Jamieson DJ, Honein MA, Petersen LR. 2016 Zika virus and birth defects–reviewing the evidence for causality. N. Engl. J. Med. **374**(20), 1981-1987. (doi: 10.1056/NEJMsr1604338)

[6] Dick GWA, Kitchen SF, Haddow AJ. 1952 Zika virus. (I). isolations and serological specificity. Trans. R. Soc. Trop. Med. Hyg. **46**(5), 509-520. (doi: 10.1016/0035-9203(52)90042-4)

[7] Smithburn KC. 1952 Neutralizing antibodies against certain recently isolated viruses in the sera of human beings residing in East Africa. J. Immunol. **69**(2), 223-234.

[8] Hayes EB. 2009 Zika virus outside Africa. Emerg. Infect. Dis. **15**(9), 1347-1350. (doi: 10.3201/eid1509.090442)

[9] Musso D, Nilles EJ, Cao-Lormeau VM. 2014 Rapid spread of emerging Zika virus in the Pacific area. Eur. J. Clin. Microbiol. **20**(10), 595-6. (doi: 10.1111/1469-0691.12707)

[10] Gao D, Lou Y, He D, Porco, Travis C, Kuang Y, Chowell G, Ruan S. 2016 Prevention and control of Zika fever as a mosquito-borne and sexually transmitted disease. Sci. Rep. **6**, 28070. (doi: 10.1038/srep28070)

[11] He D, Gao D, Lou Y, Zhao S, Ruan S. 2017 A comparison study of Zika virus outbreaks in French Polynesia, Colombia and the State of Bahia in Brazil. Sci. Rep. **7**(1), 273. (doi: 10.1038/s41598-017-00253-1)

[12] CDC. Emergency operations center moves to highest level of activation for zika response, Febraury 3, 2016. `http://www.cdc.gov/media/releases/2016/s0208-zika-eoca-activation.html`. (Accessed on February 26, 2016)

[13] Atkinson B, Hearn P, Afrough B, Lumley S, Carter D, Aarons EJ, Simpson AJ, Brooks TJ, Hewson R. 2016 Detection of Zika virus in semen. Emerg. Infect. Dis. **22**(5), 940. (doi: 10.3201/eid2205.160107)

[14] Musso D, Roche C, Nhan TX, Robin E, Teissier A, Caolormeau VM. 2015 Detection of Zika virus in saliva. J. Clin. Virol. **68**, 53-55. (doi: 10.1016/j.jcv.2015.04.021)

[15] Gourinat AC, OĆonnor O, Calvez E, Goarant C, Dupontrouzeyrol M. 2015 Detection of Zika virus in urine. Emerg. Infect. Dis. **21**, 84C6. (doi: 10.3201/eid2101.140894)

[16] Bewick S, Fagan W, Calabrese J, Agusto F. 2016 Zika virus: endemic versus epidemic dynamics and implications for disease spread in the americas. BioRxiv 041897.

[17] Kucharski AJ, Sebastian FE, Rosalind M, Henri-Pierre M, John EW, Nilles EJ. 2016 Transmission dynamics of Zika virus in island populations: A modelling analysis of the 2013C14 French Polynesia outbreak. Plos Neglect. Trop. D. **10**(5), e0004726. (doi: 10.1371/journal.pntd.0004726)

[18] Bastos LS, Villela DA, Carvalho LMD, Cruz OG, Gomes MF, Durovni B, et al. 2017 Zika in Rio de Janeiro: assessment of basic reproductive number and its comparison with dengue. Epidemiol. Infect. **145**(8), 1649-1657. (doi: 10.1017/S0950268817000358)

[19] Wang L, Zhao H, Oliva SM, Zhu H. 2017 Modeling the transmission and control of Zika in Brazil. Sci. Rep. **7**(1). (doi: 10.1038/s41598-017-07264-y)

[20] Agusto FB, Bewick S, Fagan WF. 2017 Mathematical model for Zika virus dynamics with sexual transmission route. Ecol. Complex. **29**, 61-81. (doi: 10.1016/j.ecocom.2016.12.007)

[21] Pastor-satorras R. 2000 Epidemic spreading in scale-free networks. Phys. Rev. Lett. **86**(14), 3200-3203. (doi: 10.1103/PhysRevLett.86.3200)
[22] Newman ME. 2002 Spread of epidemic disease on networks. Phys. Rev. E **66**, 016128. (doi: 10.1103/PhysRevE.66.016128)
[23] Gómez-Gardeñes J, Latora V, Moreno Y, Profumo E. 2008 Spreading of sexually transmitted diseases in heterosexual populations. P. Natl. Acad. Sci. USA **105**, 1399C404. (doi: 10.1073/pnas.0707332105)
[24] Zhang X, Shan C, Jin Z, Zhu H. 2018 Complex dynamics of epidemic models on adaptive networks[J]. J. Differ. Equations. (doi.org/10.1016/j.jde.2018.07.054)
[25] World bank. 2016. `http://wdi.worldbank.org/table/2.1`.
[26] World-Bank-Group. 2016 Population, female (% of total). `https://data.worldbank.org/indicator/SP.POP.TOTL.FE.ZS?locations=CR`.
[27] Saad-Roy CM, Driessche PVD, Ma J. 2016 Estimation of Zika virus prevalence by appearance of microcephaly. BMC Infect. Dis. **16**(1), 754. (doi: 10.1186/s12879-016-2076-z)
[28] Mcmeniman CJ, Lane RV, Cass BN, Fong AWC, Sidhu M, Wang YF, OŃeill SL. 2009 Stable introduction of a life-shortening wolbachia infection into the mosquito aedes aegypti. Science **323**(5910), 141-144. (doi: 10.1126/science.1165326)
[29] Laumann EO. 1995 The social organization of sexuality: sexual practices in the United States. Jama. J. Am. Med. Assoc. **274**(7), 535-7. (doi: 10.1001/jama.1995.03520320085050)
[30] Baumle AK. 2013 International handbook on the demography of sexuality. International Handbooks of Population, 5.
[31] Newman M E J. 2010 Networks: an introduction. Oxford University Press.
[32] Haario H, Laine M, Mira A, Saksman E. 2006 DRAM: efficient adaptive MCMC. Statistics & Computing **16**(4):339-354. (doi: 10.1007/s11222-006-9438-0)
[33] Gamerman D, Lopes HF. 2006 Markov chain Monte Carlo: stochastic simulation for Bayesian inference. Chapman and Hall/CRC.
[34] Zika virus data from PAHO. `https://www.paho.org/hq/index.php?option=com_content&view=article&id=12390&Itemid=42090&lang=en`.
[35] Whelan H. Nature tourism. 1988 Environmental Conservation, 15(2): 182-182.
[36] Ikejezie J, Shapiro CN, Kim J, Chiu M, Almiron M, Ugarte C, Espinal MA, Aldighieri S. 2017 Zika virus transmission - region of the Americas, May 15, 2015-December 15, 2016. Am. J. Transplant. **17**(6), 1681. (doi: 10.15585/mmwr.mm6612a4)
[37] Blanke J, Chiesa T. 2013 The travel & tourism competitiveness report. The World Economic Forum. 2013.
[38] Van d DP, Watmough J. 2002 Reproduction numbers and sub-threshold endemic equilibria for compartmental models of disease transmission. Math. Biosci. **180**(1-2), 29-48. (doi: 10.1016/S0025-5564(02)00108-6)
[39] Anderson R, May R. 1992 Infectious diseases of humans: Dynamics and control, Oxford science publications.
[40] Iman RL, Helton JC, Campbell JE. 1981 An approach to sensitivity analysis of computer models: Part IIIranking of input variables, response surface validation, distribution effect and technique synopsis. J. Qual. Technol. **13**(3), 174-183. (doi: 10.15585/mmwr.mm6612a4)
[41] Costa Rica Prostitution.`https://www.costaricantimes.com/costa-rica-prostitution/214`.
[42] Chandra A, Copen CE, Mosher WD. 2013 Sexual behavior, sexual attraction, and sexual identity in the united states: data from the 2006-2010 national survey of family growth. In International Handbook on the Demography of Sexuality, Springer 45C66.
[43] Zhang J, Jin Z, Chen Y. 2013 Analysis of sexually transmitted disease spreading in heterosexual and homosexual populations. Math. Biosci. **242**(2), 143-152. (doi: 10.1016/j.mbs.2013.01.005)
[44] Li S, Jin Z. 2015 Dynamic modeling and analysis of sexually transmitted diseases on heterogeneous networks. Physica A **427**, 192-201. (doi: 10.1016/j.physa.2015.01.059)
[45] Ferrariś solution. `https://en.wikipedia.org/wiki/Quartic_function#Ferrari's_solution`.
[46] Fan, S. 1989 A new extracting formula and a new distinguishing means on the one variable cubic equation.